Viscoelastic Properties of Artificial Pneumatic Muscle

Ing. Zdeněk Varga

Department of Applied Cybernetics, Technical University of Liberec, Sudentská 2,
461 17 Liberec, E-mail: zdenek.varga@gmail.com

M.Sc. Petri Keski-Honkola

Engineering design and Production, Aalto University, P. O. Box 14400, 00076 Espoo, Finland,
E-mail: petri.keski-honkola@aalto.fi

Abstract

An artificial pneumatic muscle is a hollow airproof actuator that is made out of fiber-reinforced rubber tube attached to metal fittings at each end. Muscle can produce pulling force as a function of contraction and pressure. This kind of actuator can be used to generate changes in displacement, generate vibration or damp external forces. Behavior of artificial muscles can be described using the knowledge that muscle tends to find a position with lowest energy during the loading process.

Modeling of this kind of muscle system is difficult because it has built-in nonlinearities from pneumatic medium and muscle material. The material viscoelasticity that can be described as force hysteresis, causes energy loss during loading and relaxing of the muscle. Muscle composite material elasticity also affects muscle volume and makes it a function of both pressure and contraction.

The aim of this paper is to describe the behavior of the muscle fiber composite material. The measurements in this paper show muscle material viscoelastic behavior in different stretching angles in relation to fiber directions and the dissipation of energy during the measurement cycle. These measurements were made with different frequencies in a room temperature.

KEYWORDS: artificial pneumatic muscle, damping force, tensile test

1. Introduction

Mathematical model of an artificial pneumatic muscle consists of pressurized air inside the muscle and the viscoelastic properties of base material of the muscle. While describing rubber behavior mathematically, concept of 'strain energy density' is used [1]. This approach is also used while describing muscle material behavior in this work. Mechanical properties of this material were measured and analyzed. This was done on three samples of rubber which were cut from a muscle (in three main directions) according the standard ČSN ISO 37 [2]. Measurement of mechanical properties of rubber was made by a tensile strain test to find out optimal parameters for the dynamic tests.

2. Geometrical analysis of pneumatic muscles material

Muscle selected for measurements in this article was made by Festo company and has an outer diameter 24 [mm]. Previous research made by one of the authors of this paper [3] focused on muscle geometry with the same outer diameter used here. Measured parameters were the angle between braided threads and cylinder axis θ, thickness of the shell t_k, diameter of thread d_t and dimensions between the threads and shell [**fig. 1** and **2**].

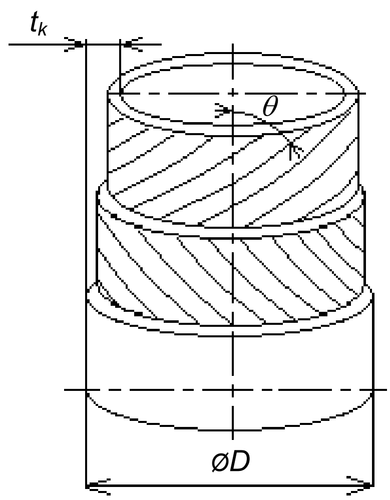

Figure 1: Structure and dimension of fiber-reinforced circular tube

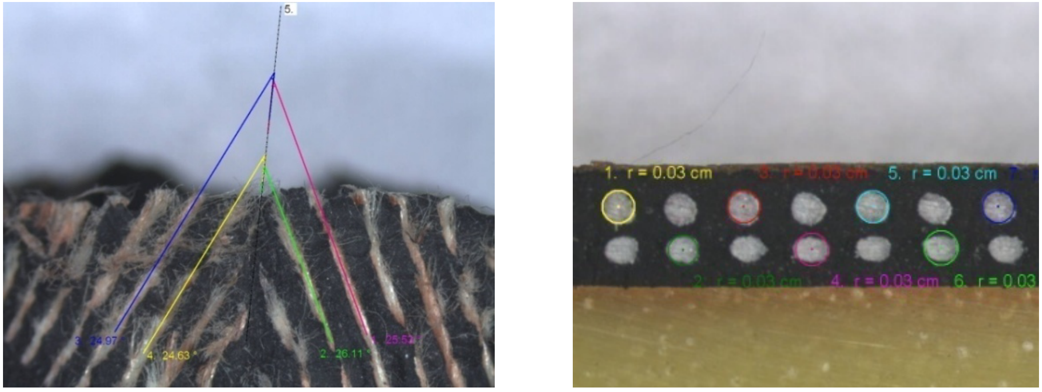

Figure 2: Measurement of the angle between muscle and axis of the muscle on the left and measurement of the diameter of fiber on the right

Data from dimension analysis is summarized in the **Tab. 1**. In the analysis of muscle material it is important to determine the angle between braided threads and the muscle axis. The measured angle *θ* corresponds to the situation when the muscle is unpressurized and at nominal diameter and length.

Table 1		
Angle of the threads	θ [°]	25
Thickness of the shell	t_k [mm]	2
Diameter of the muscle	D [mm]	24
Diameter of the thread	d_t [mm]	0,3

Table 1: Dimensions of the muscle

3. Description of rubber samples

Based on previous geometry measurement of the angle *θ,* three rubber samples were cut according to the standard ČSN ISO 37, from which type 3 configuration was chosen.

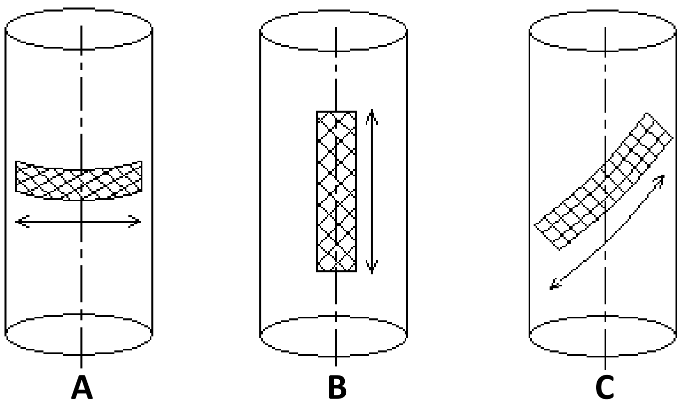

Figure 3: Orientation of the rubber samples in relation to muscle shell

The samples of rubber were made in relation to three main directions of orientation of thread and are shown in **Fig. 3**. The next important step in preparing of the samples was to glue the harder rubber pieces at the ends. These pieces strengthen the connection between sample and loading machine clamps, preventing any unwanted slipping.

Figure 4: Shape of rubber samples according to the standard ČSN ISO 37 type 3

4. Loading of rubber samples

A complex analysis of the base muscle material requires loading tests in three main directions as shown in Fig. 3. Directions are **A** – perpendicular, **B** – lengthwise, and **C** – in direction of reinforced threads. At the beginning of testing, there was no information about material properties and a preliminary calibration test was needed to find out proper dynamic loading conditions.

4.1. Mechanical properties of samples – tensile test

A tensile test was made to find out proper dynamic loading conditions for the material in question. Test was made on each group of the samples and the results are shown in **Fig 5**. For the measurements **TIRA test 2810** test machine was used. In the Fig. 5 three graphs from the measurements are shown, each showing a macroscopic process. The process starts after yield strength is achieved, after that force goes dramatically down.

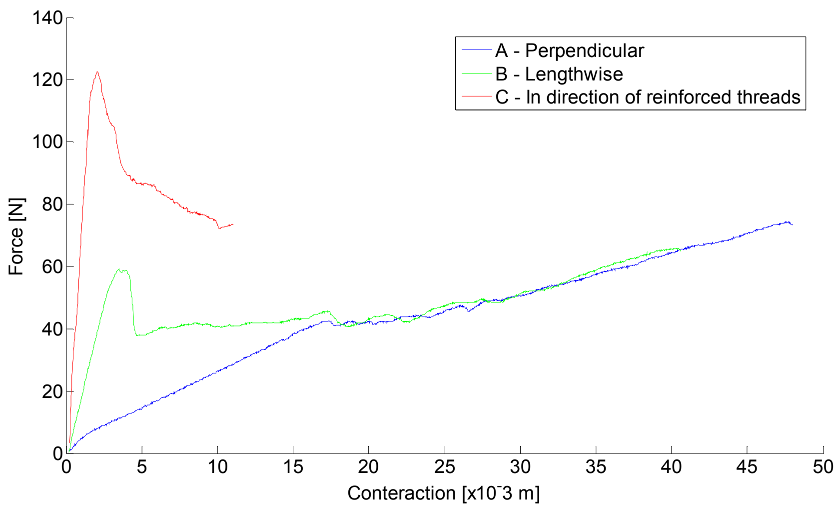

Figure 5: Tensile test of samples with different orientation of reinforced fiber

4.2. Proposed condition for loading the samples

Based on the mechanical material properties achieved from test described previously, it was possible to determine proper conditions for dynamic sample loading. Planned measurements were done as first overview of mechanical properties of samples with different fibre orientation. Results showed that force controlled sinusoidal test cycle should be chosen for dynamic tests instead if position controlled test.

The parameters for dynamic tests were chosen according to the results of preliminary tensile tests presented in Fig. 5. and following parameters were then used.

A – vertical direction 20 ± 10 [N]

B – lengthwise direction 30 ± 10 [N]

C – direction of reinforced threads 70 ± 10 [N]

Dynamic loading was made at frequencies $f \in \{0,5;\ 1;\ 2;\ 3;\ 4;\ 5\}$ Hz and before each measurements a pre-run was made for "rubber training" with a frequency of f=0,5 Hz to get rid of the Mullins effect.

5. Methodology of measurement evaluation

Methods described in the articles [4] and [5] were used for the analysis of measured data. In these articles dissipation caused by damping was evaluated from curve integral of damping force F_d. described by equation 1.

$$W_{\mathrm{d}} = \oint F_{\mathrm{d}}\,\mathrm{d}x \tag{1}$$

In this paper energy dissipated by damping was determined by calculating hysteresis loop area from the measurements using equation 2. Measurements were used instead of theoretical model because too little is known about the muscle material properties. Work caused by damping force (dissipated energy) was determine in this case by counting the volume of area inside the polygon with the tops [6] $A_1 = [x_1, y_1], A_2 = [x_2, y_2] \ldots A_n = [x_n, y_n]$.

$$W_d = \frac{1}{2}\left\| \begin{vmatrix} x_1, x_2 \\ y_1, y_2 \end{vmatrix} + \begin{vmatrix} x_2, x_3 \\ y_2, y_3 \end{vmatrix} + \ldots + \begin{vmatrix} x_n, x_1 \\ y_n, y_1 \end{vmatrix} \right\| \tag{2}$$

6. Analysis of measured data

During the measurements with samples from group **A,** it became evident that the test sample was partly destroyed so that threads were separated from it. This made the measurement flawed. Due to this phenomenon, which happened to all similar samples, special samples were made that had a constant width of 10mm.

The measured data from the new samples of rubber could not be used in the analysis because these samples were no longer comparable with the originals. It was also impossible to estimate the exact effect of the modifications due to the fact that base material was nonlinear and that the loading of samples was chosen to be force controlled.

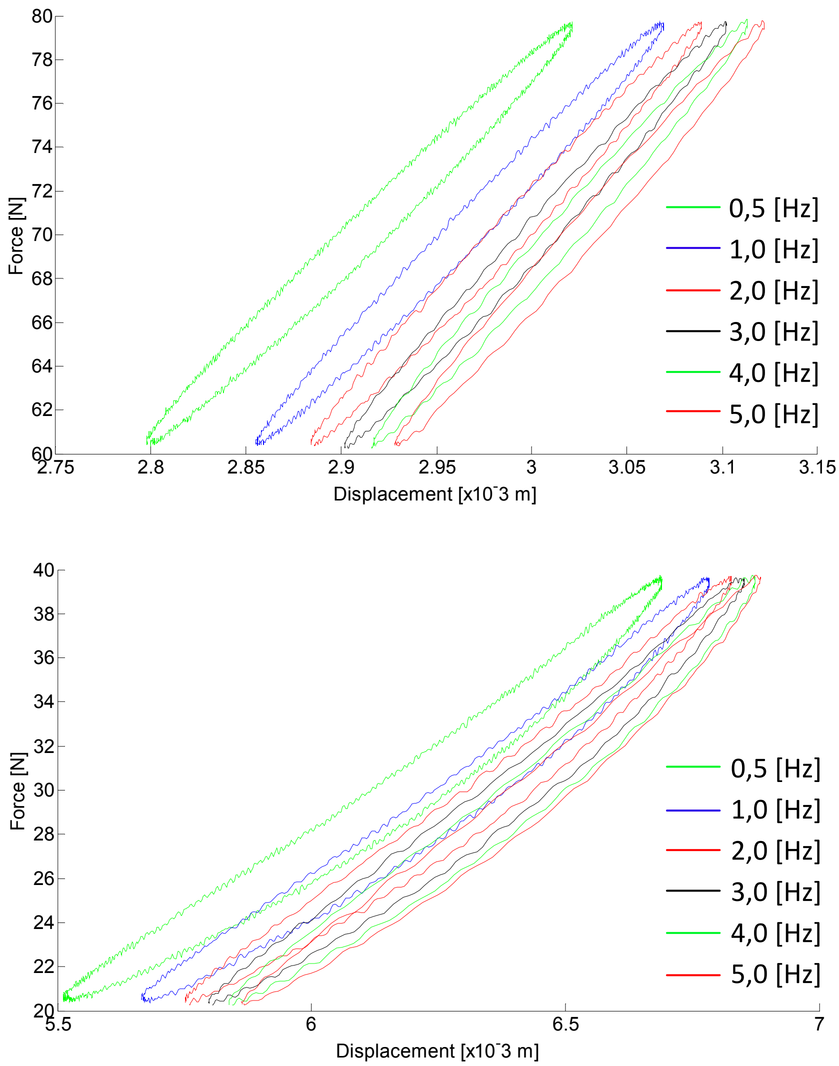

Figure 6: Dependence of force on the frequency – measured data. Upper graph shows measurements with a sample type C and lower graph sample type B.

Fig. 6 shows the measured force compared to sample strain at different testing frequencies. As explained before only sample types B and C could be used. In sample B rubber was pulled in a "normal" muscle axial direction. Sample C is cut so that the pulling force is parallel to the fibers. Damping energy was calculated from hysteresis loops using formula 2. Results from different frequencies for both samples are presented in **fig. 7**.

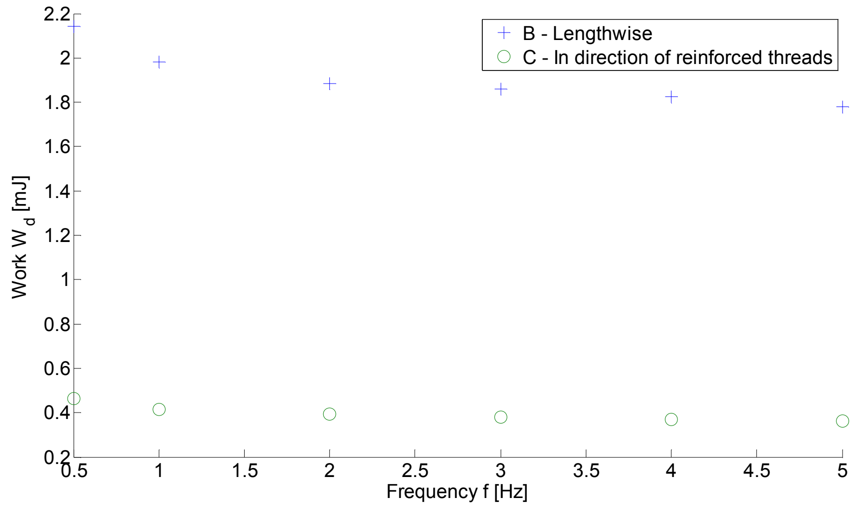

Figure 7: Dependency of energy loss due to damping and the frequency

7. Discussion

To obtain a better knowledge of pneumatic artificial muscle behaviour, more information of the muscle material was needed. For this reason a series of tests were made for samples cut from an actual muscle shell. Because muscle shell composes of rubber and non-elastic fibers samples behave differently when loading force direction changes in respect to fibers.

Three differently oriented samples were prepared and a tensile test was made. It was found out that type-A samples were not testable because cutting around the muscle severed the fibers to short pieces that were separated from rubber when the sample was loaded. For this reason type A samples were dismissed.

From type B and C tensile test it can be seen that after 19% of pulling, muscle material starts to fail. When force is parallel to muscle fibers, sample stood up to two times the force compared with situation where sample was pulled in muscle axial direction. Stiffness of the sample C was about 100 N/mm while sample A had stiffness of 20 N/mm. Reason for this is that the fibers turn inside the rubber when force is directional to muscle axis and rubber takes most of the load in the beginning. When sample is pulled in the parallel to the fibers the load is placed mainly on them and rubber has a minor role.

After determining proper dynamic loading conditions with these static loading tests, samples were tested with sinusoidal displacement loading where displacement and loading force were measured. Tests were made with different frequencies from 1 to 5 Hz in one hertz intervals. From the resulting hysteresis curves damping work with different frequencies could be calculated as presented in Fig. 7. It can be seen that type B sample lost almost ten times more energy due damping than sample C with the same 20 N of differential loading force. Reason for this is that in sample B the rubber dominates as a material and in sample C the fibers properties are dominant.

8. Conclusion

The main contribution of this paper is knowledge of the force that is needed for damaging the structures inside the samples made of the artificial pneumatic muscle shell. The measured tear forces for samples are presented in Fig. 5. From the mentioned graph is possible to see elongation for three main reinforced fibre directions which may be very helpful for future testing with position control. These measurements may also be used to build a model of muscle material damping. Another application is a model that could estimate volume change caused by material elasticity during pressurizing and loading of a muscle.

9. Acknowledgements

Authors would like to give a special recognition to Dr. David Cirkl for his help with the measurements and for consultation with the results.

10. Bibliographical References

/1/ Klute, G. K. and Hannaford, B., 1998a, “Fatigue characteristics of McKibben artificial muscle actuators,”Proceedings, IEEE/RSJ 1998 International Conference on Intelligent Robotic Systems (IROS ’98),Victoria BC, Canada, Vol. 3, pp. 1776-1781

/2/ Rubber, vulcanized or thermoplastic – Determination of tensile stress-strain properties ČSN ISO 37, Český normalizační úřad, 2006, pp. 1–28

/3/ Varga. Z & Moučka. M. January 2009. Mechanic of Pneumatic Artificial Muscle, Journal of Applied Science in the Thermodynamics and Fluid Mechanics, Vol. 3, No 2/2009, Czech Republic, pp. 1–6, ISSN 1802-9388

/4/ Cirkl, D. Modelling of damping force of dynamically loaded specimenn of polyurethane foam in dependence on its density. Shock and Vibration 17 (2010), pp. 373–381, ISSN 1070-9622

/5/ Cirkl, D. Modelling of damping force of polyurethane foam in dependence on its temperature. 10th International conference on Vibrational Problems, Sept. 5th-8th 2011. Springer proceedings in Physics 139, pp. 664–669, ISBN 0930-8989

/6/ Rektorys. K. Přehled užité matematiky I. Karel Rektorys a spolupracovníci, Praha, 1995, Czech Republic, pp. 165, ISBN 80-85849-92-5

11. Symbols

W_d	work of damping force	J
F_d	damping force	N
f	Frequency	Hz